Multi-time Scale Energy Management Strategy of Aggregator Characterized by Photovoltaic Generation and Electric Vehicles

Junjie Hu, *Member*, *IEEE*, Huayanran Zhou, *Student Member*, *IEEE*, Yang Li, Peng Hou, *Member*, *IEEE*, and Guangya Yang, *Senior Member*, *IEEE*

***Abstract*—The increasing number of photovoltaic (PV) generation and electric vehicles (EVs) on the load side has necessitated an aggregator (Agg) in power system operation. In this paper, an Agg is used to manage the energy profiles of PV generation and EVs. However, the daily management of the Agg is challenged by uncertain PV fluctuations. To address this problem, a robust multi-time scale energy management strategy for the Agg is proposed. In a day-ahead phase, robust optimization is developed to determine the power schedule. In a real-time phase, a rolling horizon-based convex optimization model is established to track the day-ahead power schedule based on the flexibilities of the EVs. A case study indicates a good scheduling performance under an uncertain PV output. Through the convexification, the solving efficiency of the real-time operation model is improved, and the over-charging and over-discharging problems of EVs can be suppressed to a certain extent. Moreover, the power deviation between day-ahead and real-time scheduling is controllable when the EV dispatching capacity is sufficient. The strategy can ensure the flexibility of the Agg for real-time operation.**

***Index Terms*—Aggregated electric vehicle (EV), aggregator (Agg), photovoltaic (PV), robust optimization, convex optimization.**

I. Introduction

In recent years, the penetration of renewable energy sources (RESs) and distributed energy sources (DERs) on the load side has increased significantly [1]. As an intermediate entity between the end users and the power system operator, an aggregator (Agg) has been proposed to manage the energy of local RESs and DERs [2], and will play an important role in future smart grids. However, the power outputs of RESs have uncertain characteristics [3], [4], causing challenges in the energy management of the Agg. Employing the flexibility of electric vehicles (EVs) is widely considered as an economical and efficient solution to the problem [5], [6]. Thus, this motivation has spurred researchers to develop an optimal energy management strategy for EVs with a high penetration of RESs.

In terms of system energy management, two mainly used time scales are day-ahead and real-time. For the day-ahead optimization, as some system parameters are unknown before the day, the prediction-based day-ahead optimization will be challenged by uncertainty. Multiple scenario based stochastic programming and robust optimization are the effective methods for dealing with the uncertainty in day-ahead optimization. To maximize the consumption of renewable energy, the optimal charging management of EV fleets is described in [7] for multiple scenarios based on stochastic programming. The uncertainties presented by the numerous scenarios are processed by a Monte Carlo simulation. Both static and dynamic scenarios are considered in [8] to handle the uncertainties. Although the multiple scenario based method is widely used in modeling system uncertainties, it has potential risks if the uncertainties cannot be truly represented by the limited set of scenarios. Robust optimization (RO) control of EVs is used in [9] and [10] to reduce the impacts of RES fluctuations on scheduling. Various day-ahead energy management strategies are studied in [7]-[10]. However, challenges on how to implement those strategies in a real-time operation still remain.

In the phase of real-time operation, [11] schedules the EV charging load to match the uncertain wind energy based on a heuristic approach. The approach is not well-suited when applied to large-scale systems, owing to the inherent inefficiency of the calculations. To meet the calculation speed requirements for the coordinated charging of a large population of EVs, [12], [13] adopt a myopic EVs charging strategy to smooth the load curve in RES-connected systems. Nevertheless, the flexibility of the EVs will decrease as the scheduling process proceeds. As a different approach from the real-time scheduling strategies in [11]-[13], [14] establishes a mechanism incorporating estimated day-ahead information to

Manuscript received: July 13, 2019; accepted: April 9, 2020. Date of Cross-Check: April 9, 2020. Date of online publication: July 9, 2020.

This work was supported in part by the National Natural Science Foundation of China (No. 51877078) and the Fundamental Research Funds for the Central Universities (No. 2018MS012).

J. Hu, H. Zhou, and Y. Li are with the State Key Laboratory of Alternate Electrical Power System with Renewable Energy Sources, North China Electric Power University, Beijing 102206, China (e-mail: junjiehu@ncepu. edu. cn; zhouhuayanran@163.com; liyangncepu@163.com).

P. Hou (corresponding author) is with the SEWPG European Innovation Center, Aarhus, Denmark (e-mail: houpeng@shanghai-electric.com).

G. Yang is with the Center for Electric Power and Energy, Technical University of Denmark, Lyngby, Denmark (e-mail: gyy@elektro.dtu.dk).

DOI: 10.35833/MPCE.2019.000464

help reduce the uncertainties in the real-time scheduling stage. References [15], [16] also propose a real-time energy management of EVs with reference to useful power information from day-ahead scheduling. Taking the day-ahead scheduling results as a baseline, the real-time operation results shown in [14]-[16] still have some deviations. If the deviations can be exploited according to the operation requirements, it will be more conductive to the Agg, managing the energies of the numerous DERs.

Based on the day-ahead and real-time scheduling mechanism, a robust multi-time scale energy management strategy for an Agg, distributed photovoltaic (PV), and EVs is proposed. The main contributions of this paper are twofold. Firstly, a day-ahead robust optimization model which can manage the inaccuracy of the forecasted PV output is established, to minimize the cost of the Agg in the electricity market. As a risk-averse approach to modeling uncertainties, robust optimization has advantages in managing the stochastic fluctuation of RESs. Secondly, a real-time convex optimization model is established to track the day-ahead scheduled power plan. The developed convexification method is easy to implement. Using the convex optimization model, the power deviation between the day-ahead and real-time phases can be adjusted according to operation demand. Moreover, from the perspective of EV users, the over-charging and over-discharging problems of each EV can be suppressed.

The remainder of this paper is organized as follows. Section II explains the overall system energy management strategy. The proposed day-ahead and real-time optimal scheduling model is provided in Section III. Section IV presents the simulation setup and results. Conclusions are summarized in Section V.

II. Multi-time Scale Energy Management Strategy

The Agg energy management framework consists of the electricity market, the Agg, grid-connected EVs, PV generation, and regular load, as shown in Fig. 1. Agg aggregates and schedules PV, EVs, and regular load.

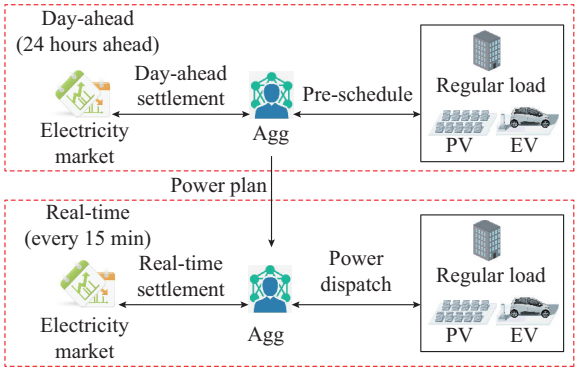

Fig. 1. Illustration of multi-time scale energy management process.

As an electricity price taker, the Agg first participates in the day-ahead electricity market to import or export the electricity, and then aims to track the day-ahead power schedule in real time. It is presumed that Agg will be punished by the utility if the deviations exceed a certain percentage of the day-ahead settlement. In addition, we assume that it is not economical for the Agg to reschedule the energy via participating in the real-time energy market. The process of multi-time scale energy management is as follows.

The day-ahead operation is carried out 24 hours before the operation day. The Agg makes a power schedule for the EV, to reduce the cost of electricity consumption based on predicted electricity prices, PV outputs, EV charging requirements, and regular load. However, the stochastic features of PVs and EVs cause the deviations between the plan and reality. To reduce unexpected electricity costs and avoid being punished, it is necessary to carry out a real-time operation.

During the real-time operation, the Agg utilizes the flexibility of the EVs. In particular, it implements optimization scheduling for the charging/discharging power of connected EVs every 15 min to track the day-ahead power plan based on the actual behavior of the EVs, PV, and regular load.

For comparative analysis, two evaluation indexes for a scheduling strategy in a real-time operation phase are defined in (1) and (2), respectively.

$$e_t = (P_t^{EV} + P_t^{load} - P_t^{PV}) - P_t^{des} \tag{1}$$

$$Acc = 1 - \sum_{t \in T} |e_t| \Big/ \sum_{t \in T} |P_t^{des}| \tag{2}$$

where e_t is the tracking error at time step t, and is equal to the actual Agg power including the EV power P_t^{EV}, the regular load P_t^{load}, and the PV power P_t^{PV}, minus the day-ahead scheduling Agg power P_t^{des}; Acc is the tracking accuracy; and T is the total number of scheduling time steps.

III. Day-ahead and Real-time Optimal Scheduling Model for Agg

A. Day-ahead Cost Minimization Model for Agg

For the day-ahead scheduling, the Agg aims to minimize the cost of the energy exchange to the external grid. The objective function is expressed as follows. The objective of the day-ahead optimization model is to minimize the cost of the Agg.

$$\min(\lambda_t \tilde{P}_t^{Agg} \Delta t) \tag{3}$$

s.t.

$$\tilde{P}_t^{Agg} = \sum_{i \in \tilde{N}_t} (\tilde{P}_{i,t}^{d} + \tilde{P}_{i,t}^{c}) + \tilde{P}_t^{load} - \tilde{P}_t^{PV} \quad \forall t \in T \tag{4}$$

$$\underline{b}_t \le \tilde{P}_t^{Agg} \le \overline{b}_t \quad \forall t \in T \tag{5}$$

$$M_{i,t}^{d} P_{i,d}^{R} \le \tilde{P}_{i,t}^{d} \le 0 \quad \forall i \in \tilde{N}_t, t \in T \tag{6}$$

$$0 \le \tilde{P}_{i,t}^{c} \le M_{i,t}^{c} P_{i,c}^{R} \quad \forall i \in \tilde{N}_t, t \in T \tag{7}$$

$$M_{i,t}^{c}, M_{i,t}^{d} \in \{0, 1\} \quad \forall i \in \tilde{N}_t, t \in T \tag{8}$$

$$M_{i,t}^{c} + M_{i,t}^{d} = 1 \quad \forall i \in \tilde{N}_t, t \in T \tag{9}$$

$$\tilde{P}_{i,t}^{c} = \tilde{P}_{i,t}^{d} = 0 \quad \forall i \in \tilde{N}_t, t \notin [\tilde{t}_i^{arr}, \tilde{t}_i^{dep}] \tag{10}$$

$$\tilde{S}_{i,t}^{SOC} = \tilde{S}_{i,t-1}^{SOC} + \left(\tilde{\eta}^{i,c} \tilde{P}_{i,t}^{c} + \frac{\tilde{P}_{i,t}^{d}}{\tilde{\eta}^{i,d}} \right) \frac{\Delta t}{\tilde{E}_i^{cap}} \quad \forall i \in \tilde{N}_t, t \in T \tag{11}$$

$$\underline{S}_i^{SOC} \le \tilde{S}_{i,t}^{SOC} \le \overline{S}_i^{SOC} \quad \forall i \in \tilde{N}_t, t \in T \tag{12}$$

$$\tilde{S}_{i,t}^{SOC} \ge \tilde{S}_i^{SOC,des} \quad \forall i \in \tilde{N}_t, t = \tilde{t}_i^{dep} \tag{13}$$

where λ_t is the electricity price in the day-ahead market; $\tilde{P}_t^{Agg}$ is the transfer power between the Agg and grid at each time step, $\tilde{P}_t^{Agg} \ge 0$ represents the power consumption of the Agg, and $\tilde{P}_t^{Agg} \le 0$ represents the export power from the Agg to the grid; Δt is the length of each time step in the day-ahead market; $\tilde{P}_{i,t}^{c} \ge 0$ and $\tilde{P}_{i,t}^{d} \le 0$ are the charging and discharging decision variables of the i^{th} EV at time step t, respectively; $\tilde{N}_t$ is the predicted number of grid-connected EVs at time step t; $\tilde{P}_t^{load}$ is the predicted power of the regular load; $\tilde{P}_t^{PV}$ is the predicted PV output power; $\overline{b}_t$ and $\underline{b}_t$ are the upper and lower limits of the Agg energy exchange to the external grid, respectively; $P_{i,c}^{R}$ and $P_{i,d}^{R}$ are the rated charging and discharging power of the i^{th} EV, respectively; $M_{i,t}^{c}$ and $M_{i,t}^{d}$ are the complimentary 0-1 binary variables, and are used to guarantee that the charging and discharging of the i^{th} EV are mutually exclusive; $\tilde{t}_i^{arr}$ and $\tilde{t}_i^{dep}$ are the predicted arrival and departure time of the i^{th} EV, respectively; $\tilde{S}_{i,t}^{SOC}$ is the state of charge (SOC) of the predicted i^{th} EV at time step t; $\tilde{E}_i^{cap}$ is the capacity of the i^{th} EV; $\tilde{\eta}^{i,c}, \tilde{\eta}^{i,d} \in (0, 1)$ are the efficiencies of the charging and discharging processes, respectively; $\underline{S}_i^{SOC}$ and $\overline{S}_i^{SOC}$ are the lower and upper limits of the SOC of the i^{th} EV, respectively; and $\tilde{S}_i^{SOC,des}$ is the predicted desired SOC of the i^{th} EV at the departure time.

Notably, the day-ahead optimal dispatching model above does not consider the uncertainty, and the optimized solution may fail to cope with the uncertain fluctuations of PV output. Robust optimization has advantages in managing uncertainties in which the probability distribution of uncertain parameters is unknown, and only the fluctuation range of the parameters is given. The uncertain sets are used to describe the fluctuation of the PV output. As long as the uncertain parameters are within the range of the uncertain sets, the feasibility of the solution can be guaranteed [17]. The deviation between the actual output and predicted output of PV is taken as an uncertain variable, and a box uncertainty set is used to describe the uncertainty:

$$\begin{cases} P_t^{PV} = \tilde{P}_t^{PV} + \xi_t \\ \underline{\xi}_t \le \xi_t \le \overline{\xi}_t \end{cases} \tag{14}$$

where P_t^{PV} and $\tilde{P}_t^{PV}$ are the actual and predicted outputs of the PV generation, respectively; ξ_t is the deviation between the actual and predicted outputs; and $\overline{\xi}_t$ and $\underline{\xi}_t$ are the upper and lower limits of the uncertainty, respectively.

Thus, $\tilde{P}_t^{Agg}$ in the day-ahead optimization model is formulated as:

$$\tilde{P}_t^{Agg} = \sum_{i \in \tilde{N}_t} (\tilde{P}_{i,t}^{d} + \tilde{P}_{i,t}^{c}) + \tilde{P}_t^{load} - P_t^{PV} = \sum_{i \in \tilde{N}_t} (\tilde{P}_{i,t}^{d} + \tilde{P}_{i,t}^{c}) + \tilde{P}_t^{load} - \tilde{P}_t^{PV} - \xi_t \quad \forall t \in T \tag{15}$$

The introduction of the uncertain variable ξ_t makes it difficult to solve the optimization model. We formulate an equivalent model by using duals of (14) and (15) [18], leading to the following tractable representation:

$$\max_{\xi_t} (-\xi_t) \tag{16}$$

s.t.

$$\begin{cases} \xi_t \le \overline{\xi}_t \lambda_\xi^+ \\ -\xi_t \le -\underline{\xi}_t \lambda_\xi^- \end{cases} \tag{17}$$

where λ_ξ^+ and λ_ξ^- are the dual variables which are equivalent to Lagrange multipliers. The optimization (16) and (17) is further formulated as:

$$\min_{\lambda_\xi^+, \lambda_\xi^-} (\overline{\xi}_t \lambda_\xi^+ - \underline{\xi}_t \lambda_\xi^-) \tag{18}$$

s.t.

$$\lambda_\xi^+ - \lambda_\xi^- = -1 \quad \lambda_\xi^+ \ge 0, \lambda_\xi^- \ge 0 \tag{19}$$

From the weak duality of dual theory, any feasible λ_ξ^+ and λ_ξ^- in (18) and (19) will be the upper bound for the maximization of (16) and (17). Hence, we can drop the minimization term in (18) and (19), and the achieved solution for both the primal and dual will be the same:

$$\tilde{P}_t^{Agg} = \sum_{i \in \tilde{N}_t} (\tilde{P}_{i,t}^{d} + \tilde{P}_{i,t}^{c}) + \tilde{P}_t^{load} - \tilde{P}_t^{PV} + \overline{\xi}_t \lambda_\xi^+ - \underline{\xi}_t \lambda_\xi^- \tag{20}$$

$$\lambda_\xi^+ - \lambda_\xi^- = -1 \quad \forall t \in T \tag{21}$$

$$\begin{cases} \lambda_\xi^+ \ge 0 \quad \forall t \in T \\ \lambda_\xi^- \ge 0 \quad \forall t \in T \end{cases} \tag{22}$$

Therefore, a robust optimization model without uncertain variables in (3), (5), (6)-(13), and (20)-(22) is established for this day-ahead schedule. After solving the day-ahead model, the power plan for the Agg can be obtained, and is denoted as P_t^{des}, which will serve as the targeted baseline in the real-time operation.

$$P_t^{des} = \tilde{P}_t^{Agg} \quad \forall t \in T \tag{23}$$

B. Real-time Operation of Agg for EVs

In real-time operation, based on the actual behavior of the EVs, load, and PV in real-time operation, the Agg employs the flexibility in the charging and discharging of EVs in the vehicle-to-grid mode to track the expected power plan. Therefore, as defined in (1), the following equation holds for each time step in the real-time operation if the tracking error is 0:

$$\left[\sum_{i \in N_t} (P_{i,t}^{c} + P_{i,t}^{d}) + P_t^{load} - P_t^{PV} \right] - P_t^{des} = 0 \tag{24}$$

where $\sum_{i \in N_t} (P_{i,t}^{c} + P_{i,t}^{d})$ is the total EV power, which is equal to P_t^{EV} in (1); and N_t is the number of grid-connected EVs at time step t.

As the PV power and regular load do not have the flexibility, the Agg can only realize the tracking of the expected power by scheduling the charging and discharging power of

EVs. To facilitate the analysis, the expected power of the EVs is defined as:

$$P_t^{EV,des} = P_t^{des} - P_t^{load} + P_t^{PV} \tag{25}$$

where $P_t^{EV,des}$ is the expected power of the EVs at time step t. Thus, the EVs' tracking of $P_t^{EV,des}$ is equal to the Agg's tracking of P_t^{des} in the real-time operation.

Moreover, to meet the energy requirements of the EVs over a relatively long period, we use rolling horizon optimization [19]. At the beginning of each time step, the Agg carries out real-time optimization for the current time step t and the following rolling horizon $\mathcal{H}=\{t+1, t+2, ..., t+H\}$. However, only the EV dispatching power of the current time step from the optimization solutions will be actually implemented by the Agg. When the next time step arrives, the Agg carries out the real-time optimization based on the updated available information and prediction. Generally, the rolling-horizon length can be set according to practical needs such as the forecasting lead-time and/or the updating frequency. Here, the prediction horizon is selected as four time steps in real time, i.e., 1 hour. The rolling horizon-based real-time dispatching model is formulated as:

$$\min\left\{\sum_{i\in N_t}\left[(P_{i,t}^d + P_{i,t}^c) - P_t^{EV,des}\right]^2 + \sum_{\tau\in\mathcal{H}}\left[\left(P_{i,\tau}^d + P_{i,\tau}^c\right) - P_\tau^{EV,des}\right]^2\right\} \tag{26}$$

s.t.

$$0 \le P_{i,k}^c \le M_{i,k}^c P_{i,c}^R \quad \forall i \in N_t, k \in \{t,\tau\} \tag{27}$$

$$M_{i,t}^d P_{i,d}^R \le P_{i,k}^d \le 0 \quad \forall i \in N_t, k \in \{t,\tau\} \tag{28}$$

$$M_{i,k}^c, M_{i,k}^d \in \{0,1\} \quad \forall i \in N_t, k \in \{t,\tau\} \tag{29}$$

$$M_{i,t}^c + M_{i,t}^d = 1 \quad \forall i \in N_t, k \in \{t,\tau\} \tag{30}$$

$$P_{i,k}^c = P_{i,k}^d = 0 \quad \forall i \in N_t, k \notin [t_i^{arr}, t_i^{dep}] \tag{31}$$

$$S_{i,\tau}^{SOC} = S_{i,\tau-1}^{SOC} + \left(\eta^{i,c} P_{i,\tau}^c + \frac{P_{i,\tau}^d}{\eta^{i,d}}\right)\frac{\Delta t}{E_i^{cap}} \quad \forall i \in N_t \tag{32}$$

$$\underline{S}_i^{SOC} \le S_{i,k}^{SOC} \le \overline{S}_i^{SOC} \quad \forall i \in N_t, k \in \{t,\tau\} \tag{33}$$

$$S_{i,t+H}^{SOC} \ge S_{i,t+H}^{SOC,pre} \quad \forall i \in N_t \tag{34}$$

The objective function (26) consists of two parts: the objective of the current time step t, and the objective of the future time step τ, which is the time step of the rolling horizon $\mathcal{H}$. We use k to indicate the time steps from t to τ. The constraints in (27)-(34) can be explained in a similar manner as the constraints in (6)-(13). The real-time operation has a high demand for computation time. It is preferable to remove the nonlinear constraints in (27)-(34), so that the solving time of the model can be shortened. Inspired by [20], the binary variables $M_{i,k}^c$ and $M_{i,k}^d$ in (27)-(34) can be omitted by adding barrier terms to the objective function (26). Thus, the model is able to efficiently solve and satisfy (27)-(34) as well. After the above operations, the real-time convex quadratic programming model is given as:

$$\begin{cases} \min\left\{\left[\sum_{i\in N_t}(P_{i,t}^d + P_{i,t}^c) - P_t^{EV,des}\right]^2 + r_1\sum_{i\in N_t}\left|P_{i,t}^c\right| + r_2\sum_{i\in N_t}\left|P_{i,t}^d\right| + \right. \\ \left. \sum_{\tau\in\mathcal{H}}\left[\sum_{i\in N_t}(P_{i,\tau}^d + P_{i,\tau}^c) - P_\tau^{EV,des}\right]^2 + r_1\sum_{i\in N_t}\left|P_{i,\tau}^c\right| + r_2\sum_{i\in N_t}\left|P_{i,\tau}^d\right|\right\} \\ \text{s.t.} \quad 0 \le P_{i,k}^c \le P_{i,c}^R \quad \forall i \in N_t, k \in \{t,\tau\} \\ \quad P_{i,d}^R \le P_{i,k}^d \le 0 \quad \forall i \in N_t, k \in \{t,\tau\} \\ \quad P_{i,k}^c = P_{i,k}^d = 0 \quad \forall i \in N_t, k \notin [t_i^{arr}, t_i^{dep}] \\ \quad S_{i,\tau}^{SOC} = S_{i,\tau-1}^{SOC} + \left(\eta^{i,c} P_{i,\tau}^c + \frac{P_{i,\tau}^d}{\eta^{i,d}}\right)\frac{\Delta t}{E_i^{cap}} \quad \forall i \in N_t \\ \quad \underline{S}_i^{SOC} \le S_{i,k}^{SOC} \le \overline{S}_i^{SOC} \quad \forall i \in N_t, k \in \{t,\tau\} \\ \quad S_{i,t+H}^{SOC} \ge S_{i,t+H}^{SOC,pre} \quad \forall i \in N_t \end{cases} \tag{35}$$

In that regard, the added barrier terms $r_1\sum_{i\in N_t}\left|P_{i,k}^c\right|$ and $r_2\sum_{i\in N_t}\left|P_{i,k}^d\right|$, $k \in \{t,\tau\}$ in the objective function (35) have two barrier factors, $r_1 > 0$ and $r_2 > 0$. Evidently, the differences between the objective function of (26) and (35) can be ignored when r_1 and r_2 are small enough.

Then, we show that the optimal solutions of the model (35) satisfy (27)-(34).

The introduction of binary variables in (27)-(34) guarantees that the charging and discharging of the i^{th} EV are mutually exclusive in real-time operation. Thus, the key is to prove that the optimal solutions of (35) do not contain any simultaneous charging and discharging for each EV.

Assuming that for any i and t, there are two types of solutions, i.e., (36) and (37), leading to the same tracking result when the scheduling target for the i^{th} power of the EV is greater than 0. Notably, (36) is mathematically feasible, but physically impossible.

$$\begin{cases} P_{i,t}^c > 0 \\ P_{i,t}^d < 0 \end{cases} \quad \forall i \in N_t, \forall t \in T \tag{36}$$

$$\begin{cases} P_{i,t}^c > 0 \\ P_{i,t}^d = 0 \end{cases} \quad \forall i \in N_t, \forall t \in T \tag{37}$$

Assume (36) and (37) can be represented as (38) and (39), respectively. If $m_1 > 0$ and $m_2 > 0$, we have $(m_1 + m_2)m_2 \ne 0$.

$$\begin{cases} P_{i,t,1}^c = m_1 + m_2 \\ P_{i,t,1}^d = -m_2 \end{cases} \tag{38}$$

$$\begin{cases} P_{i,t,2}^c = m_1 \\ P_{i,t,2}^d = 0 \end{cases} \tag{39}$$

By substituting (38) and (39) into the objective function of (35), the i^{th} component of the objective function can be obtained from (40) and (41), respectively:

$$(m_1 - P_{i,t}^{EV,des})^2 + r_1(m_1 + m_2) + r_2 m_2 \tag{40}$$

$$(m_1 - P_{i,t}^{EV,des})^2 + r_1 m_1 \tag{41}$$

where $P_{i,t}^{EV,des}$ is the scheduling target for the i^{th} EV.

Considering that $r_1 > 0$ and $r_2 > 0$, we can infer that:

$$(m_1 - P_{i,t}^{EV,des})^2 + r_1(m_1 + m_2) + r_2 m_2 > (m_1 - P_{i,t}^{EV,des})^2 + r_1 m_1 \quad (42)$$

As the scheduling objective is to minimize the objective function of (35), (42) shows that a pair of solutions with a discharging power of 0 is the optimal solution in a set of solutions with the same tracking effect.

Similarly, the pair of solutions with the charging power of 0 is the optimal solution when the scheduling target for the i^{th} EV power is less than 0.

It has been proven that the optimal solution of model (35) does not contain any simultaneous charging and discharging for each EV, i.e., model (35) is exact in modeling the characteristics of EVs, even though there are not any 0-1 binary variables in (35). The model (35) is a convex quadratic optimization model, which can be solved more conveniently and quickly compared with the model (26)-(34).

Notably, the addition of barrier terms achieves a controllable tracking error when the dispatching capacity is sufficient. A concise proof is given below.

We assume that the dispatching capacity is sufficient at time step t, i.e., the expected power of the EVs does not exceed the upper limit of (35). As one of the charging and discharging power of the EVs is 0 at any time step, we find the minimum of (35) from the perspective of charging as (43). Similarly, from the perspective of discharging, the minimum of (35) can be obtained from (44).

$$\frac{\partial f}{\partial P_t^c} = 2(P_t^c - P_t^{EV,des}) + r_1 = 0 \quad (43)$$

$$\frac{\partial f}{\partial P_t^d} = 2(P_t^d - P_t^{EV,des}) - r_2 = 0 \quad (44)$$

where f is the objective function in (35); and $P_t^c = \sum_{i \in N_t} \left| P_{i,t}^c \right|$ and $P_t^d = \sum_{i \in N_t} \left| P_{i,t}^d \right|$ are the total charging and discharging power at time step t, respectively.

We further assume that the dispatching capacity of the EVs is sufficient. If the expected power of the EVs at time step t is within the feasible region surrounded by the constraint of (35), compared with (1), we can conclude that by rearranging (43) and (44), the minimum solution of any t satisfies $e(t) = -r_1/2$ when charging, and $e(t) = r_2/2$ when discharging, respectively. Otherwise, the minimum of (35) cannot be obtained, owing to the limitations of the feasible region. From the characteristics of the objective function (quadratic function), we can infer that the solution in this situation is $P_t^c = P_t^d = 0$, and that the absolute value of $P_t^{EV,des}$ is less than $r_1/2$ when charging, or less than $r_2/2$ when discharging. Compared with (1), the tracking error will be within $(-r_1/2, r_2/2)$ for all the solutions.

Therefore, the value of the tracking error at each time step can be controlled within $[-r_1/2, r_2/2]$ by setting the barrier factors r_1 and r_2, if the dispatching capacity is sufficient.

The addition of barrier terms in (35) also avoids the over-charging and over-discharging of each EV in real-time operation. In that regard, both r_1 and r_2 are greater than 0, so any non-zero value of charging and discharging power will increase the value of the objective function. As the objective of optimization is to minimize the objective function, it is necessary to reduce the absolute value of the charging and discharging power for any i, t. This avoids the occurrence of large charging and discharging actions in dispatching. Reference [21] suggests that EV battery degradation will be accelerated by over-charging and over-discharging actions. Thus, this approach considers the interests of EV owners, and may help to attract more EV owners to participate in dispatching.

C. Multi-time Scale Energy Management Implementation

To implement the multi-time scale energy management for the Agg, the day-ahead and real-time optimal scheduling models need to be solved in turn. The day-ahead cost minimization model for the Agg is a mixed-integer linear programming problem, whereas the real-time EV operation model is a convex quadratic programming problem. The YALMIP toolbox is combined with the intlinprog and guadprog solvers in the MATLAB2014a platform to address day-ahead and real-time optimization, respectively. Figure 2 provides a flowchart illustrating the different phases and corresponding time scales of the proposed framework and the connection of the two optimization problems.

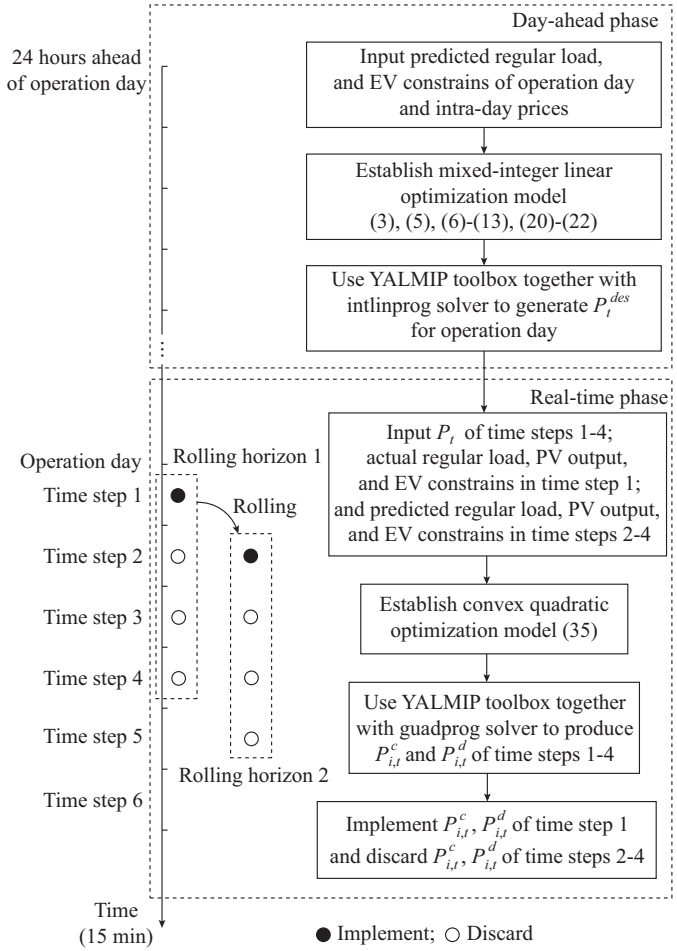

Fig. 2. Framework of multi-time scale energy management implementation.

IV. Case Studies and Discussions

A. Case Specification

In the simulation, the scheduling horizon of the simulation is from 12:00 one day to 12:00 the next day. We use an hourly interval in day-ahead optimization, and a 15 min interval in real-time operation. The rolling horizon is set to 1 hour. Figure 3 shows the predicted electricity price in the day-ahead market. The actual and expected values of the PV output are shown in Fig. 4. It is assumed that the prediction error of the PV output is ±20%. The simulation parameters for the EVs are obtained from [22]. The charging and discharging parameter settings for the EVs are listed in Table I. In all simulation scenarios, the values of the barrier factors r_1 and r_2 are set as 10, unless otherwise stated. The relationship between the values of the barrier factors and the real-time scheduling results will be discussed in Section IV-F.

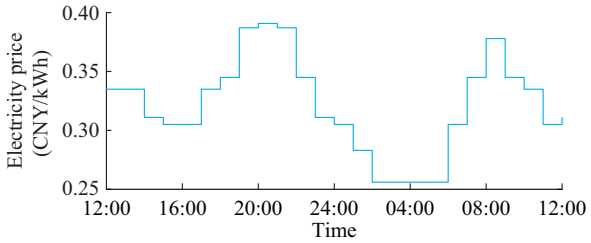

Fig. 3. Predicted electricity price in day-ahead market.

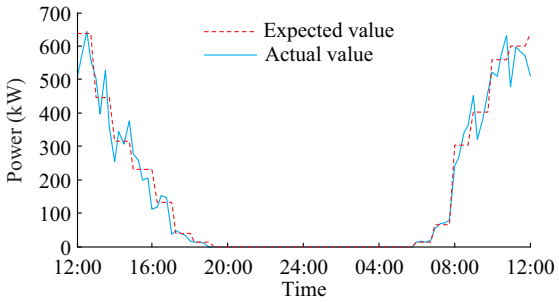

Fig. 4. Actual and expected values of PV output.

TABLE I
Parameter Settings of EV

Parameter	Value
Battery capacity (kWh)	60
Rated charging/discharging power (kW)	10
Charging/discharging efficiency	0.92
Arriving time (hour)	$N(19, 1.5^2)$
Departure time (hour)	$N(8.5, 1^2)$
Initial SOC	$N(0.6, 0.1^2)$
Desired SOC at departure time	0.85

Note: $N(x, y^2)$ stands for normal distribution, where x is the mean value, and y is the standard deviation.

B. Day-ahead Scheduling Results

The day-ahead power scheduling plan for the Agg, with different EV numbers, is shown in Fig. 5. A positive power indicates that the Agg imports the electricity from the grid, and a negative power indicates that the Agg exports the electricity to the grid.

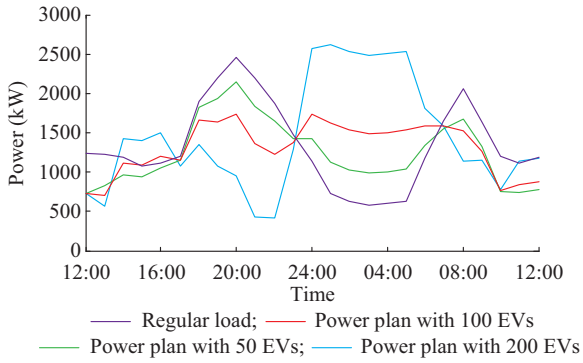

Fig. 5. Day-ahead power scheduling plan.

As shown in Fig. 5, the Agg needs to import electricity all day, owing to the large load base. To reduce the electricity purchasing cost in the day-ahead market, the Agg dispatches EVs to charge when the electricity price is low (00:00-07:00), and to discharge when the electricity price is high (17:00-23:00). At 12:00-18:00 and 06:00-12:00, the cost of purchasing power is lower than that of the regular load power. The main reason is that there is a large amount of PV power supplying loads during this period, which reduces the purchasing power of Agg from the external network. We can also see that, compared with the scheduling results for 50 EVs, the scheduled power for the Agg with 100 EVs has a better performance in load balancing and PV self-consumption, owing to a sufficient scheduling capacity. In contrast, with an excess scheduling capacity, the scheduling results for 200 EVs result in a peak/valley inversion of the regular load. Thus, we use 100 EVs as an example to carry out a detailed analysis of the real-time phase.

We calculate the cost for the Agg with different numbers of EVs participating in scheduling compared with that with uncoordinated charging of EVs, as shown in Table II. With an increasing number of EVs in the day-ahead scheduling, greater cost savings will be achieved. This is because a large number of EVs improves the scheduling capacity of the Agg, so that the Agg can respond to electricity prices more actively.

TABLE II
Cost Comparison with and Without Day-ahead Scheduling

No. of EV	Cost with scheduling (CNY)	Cost without scheduling (CNY)	Cost saving (CNY)
50	9411.2	9729.0	317.8
100	8588.2	9307.6	719.4
200	6869.7	8370.7	1501.0

C. Robustness Analysis

The uncertainties of the PV output are considered in the day-ahead scheduling, by using an RO model. A cost comparison between RO and deterministic optimization (DO) for

dispatching 100 EVs is shown in Table III. A comparison of power scheduling results between RO and DO is shown in Fig. 6. The total operation cost for Agg obtained by RO is greater than that obtained by DO. The increased cost comes from the purchase of the electricity. The electricity selling incomes from both RO and DO are 0. That is because the regular load power is much larger than the power of the connected DERs.

TABLE III
COST COMPARISON BETWEEN RO AND DO

Model	Purchasing electricity (CNY)	Selling electricity (CNY)	Total cost (CNY)
RO	8588.2	0	8588.2
DO	8300.6	0	8300.6

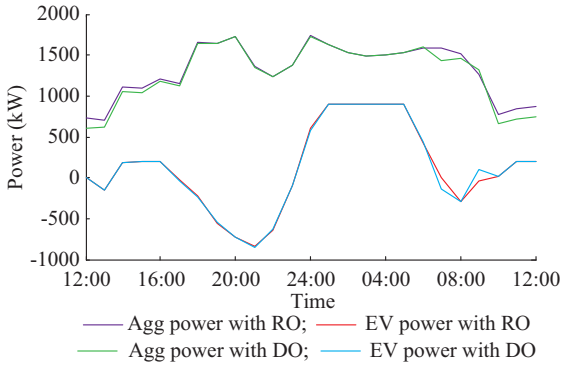

Fig. 6. Scheduling results of RO and DO.

By comparing the scheduling results for the power with RO and DO, it can be seen that the difference in power curves mainly exists in the period of PV output. The purchasing power of the Agg with RO is greater than that with DO. That is because RO fully considers the worst situation of PV output, i.e., 80% of expected PV output in this paper, to cope with uncertain PV fluctuations in real time. Sufficient electricity can be guaranteed, even if the real-time PV fluctuations are the worst case. Although the RO method increases the total operation cost of the Agg, it greatly increases the robustness of Agg under the fluctuations of PV output.

The output of EV power with RO is more conservative compared to that with DO. EVs avoid large-scale charging and discharging behavior in the period of PV output, but reserve discharging power to fill the possible insufficient PV output centrally such as in the period of 07: 00-09: 00. It should be noted that there are not many parked EVs in the period of PV output, so the power of EVs is not greatly affected by the uncertain fluctuations of PV power, resulting in small changes to the power of EV.

D. Validity of Convex Quadratic Programming in Real-time Operation

To verify the accuracy and validity of the relaxation of the non-convex constraints in the real-time model, respective simulations are conducted for a convex quadratic programming (CQP) model with barriers from objective function and linear constraint (35), a mixed integer programming (MIP) model with original objective function (26) and non-linear constraint (27)-(34), and a contrastive MIP (CMIP) model with barriers from objective function in (35) and non-linear constraint (27)-(34). Simulation results from real-time operation using CQP, MIP, and CMIP models are shown in Table IV.

TABLE IV
COMPARISONS BETWEEN CQP, MIP, AND CMIP SOLUTIONS

EVs	Objective value (kW^2)			Average solution time (s)		
	CQP	MIP	CMIP	CQP	MIP	CMIP
50	255556	70944	255556	0.21	15.24	16.47
100	417425	2429	417425	0.55	85.54	84.79
200	876943	3311	876943	1.57	676.13	655.22

The objective values obtained by the CQP and CMIP models are identical for different EV numbers. It can be inferred that the constraints (27)-(34) and the constraint of (35) are equivalent with the same objective function in (35). The value of the objective function obtained by the MIP model is less than that obtained by the CQP and CMIP models. This is because the barrier terms in (35) cause the value of the objective to increase 10 times with the output of the EVs in this simulation. In fact, the objective function of the CQP model has no physical meaning. The term of physical significance in the objective function of (35) is the square of the tracking error, which reflects the value of the tracking error. It does not matter that the objective function values of the CQP and CMIP models are quite different from those of the MIP model, as the tracking error of the EVs obtained by the CQP model is small.

Moreover, we can obtain $P^c_{i,t} P^d_{i,t} = 0$ in the solution of the CQP model, which means that each EV has only one state of charging or discharging at each time step in the optimal solution, even if there are no specific constraints in the model. Hence, the accuracy and validity of the CQP model are verified.

The average solution time of the MIP and CMIP models are almost the same, whereas the average solution time of the CQP model is much shorter than that of the MIP and CMIP models for different numbers of EVs. The effect of accelerating the solving process in the CQP model is more evident as the number of EVs increases. This is because the 0-1 binary variables introduced by constraints (27)-(34) increase the number of decision variables in the process of solving, and the introduction of the 0-1 binary variables involves a branch-and-bound solving approach. This leads to a longer solution time, especially for the quadratic objective function in this paper. After establishing the CQP model, there is no binary variable, so the solving time of the CQP model is much shorter than that of both the MIP and CMIP models. As a real-time operation must be solved in a short time, the improvement of the solution speed is meaningful. And the real-time operation of large-scale aggregated EVs is allowed over a shorter time scale.

E. Analysis of Rolling Horizon Optimization Based Real-time Control

Figure 7 shows a comparison of the tracking errors with and without the implementation of the rolling horizon optimi-

zation-based real-time operation with 100 EVs. Power deviations of the day-ahead and real-time scheduling results are presented, rather than the total power optimization results from real-time operation. Owing to the uncertainties, the transfer power between the Agg and the grid strongly deviates from the day-ahead scheduled power plan without the rolling horizon optimization based real-time operation. The large tracking error is mainly caused by the forecast error of the PV output from 06:00 to 18:00. In contrast, the tracking errors with rolling horizon optimization based real-time operation are very close to those of an optimal solution with perfect information. In the rolling horizon optimization based real-time operation, the actual charging and discharging power of EVs can be adjusted according to the actual power of PV output and load. Thus, the deviation from the day-ahead power scheduling plan can be minimized, and the uncertainties can be managed.

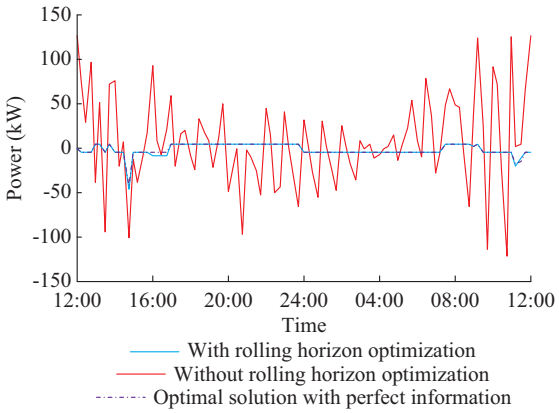

Fig. 7. Tracking error of Agg in real-time with or without rolling horizon optimization.

F. Effect of Barrier Factors on Real-time Scheduling

To illustrate the effects of the barrier factors on the real-time scheduling results, 100 EVs are respectively simulated using a series of barrier factors. Selected scenarios, with different values of barrier factors, are listed in Table V. To better demonstrate the controllability of the tracking error, it is assumed that the real-time dispatching has two stages: stage 1 is from 12:00 to 24:00, and stage 2 is from 24:00 to 12:00 the next day.

TABLE V
BARRIER FACTOR SETTING FOR DIFFERENT SCENARIOS

Scenario	Value of r_1		Value of r_2	
	Stage 1	Stage 2	Stage 1	Stage 2
A	1	1	1	1
B	10	10	10	100
C	100	100	100	100
D	8	12	12	8

As the Agg needs to track the day-ahead scheduling power plan as accurately as possible to avoid extra costs in real-time operation, it is necessary to pay attention to the tracking error in the real-time process. The tracking errors of different scenarios are shown in Fig. 8.

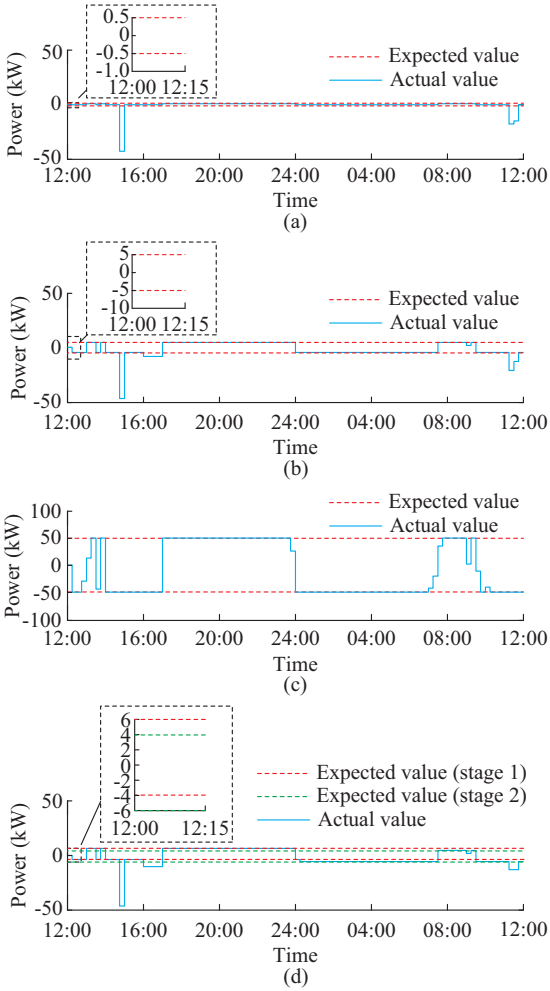

Fig. 8. e_t of Agg in real-time operation. (a) Scenario A. (b) Scenario B. (c) Scenario C. (d) Scenario D.

The tracking errors of all scenarios are within $[-r_1/2, r_2/2]$ during the majority of the time steps, even in scenario D. However, there are some tracking errors that exceed the expected range at approximately 14:45, 16:00-16:45 and 11:15-11: 30 in all scenarios except scenario C. It is noted that these errors are all negative. Taking scenario B as an example, the real-time operation results for EV charging are shown in Fig. 9.

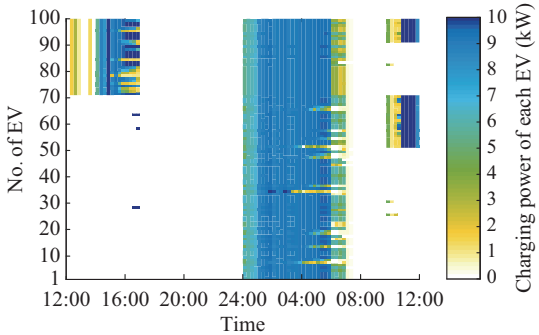

Fig. 9. Real-time operation results of EV charging in scenario B.

Compared with the day-ahead scheduled power plan, there are not enough EVs to provide sufficient capacity for real-time operation in these periods. The Agg schedules almost

all connected EVs to charge with rated power. Some EVs cannot be charged at rated power owing to SOC limitations, but it is still not enough to track the power plan, resulting in uncontrollable tracking errors. Naturally, there may be differences in the EV scheduling capacity between the real-time data and day-ahead forecast data, as EV owners are not completely obedient to the Agg. Thus, the above phenomenon is likely to occur when the obedience rate of EVs is low. In scenario C, the Agg reduces the dispatching power for each EV owing to large values of barrier factors, so the dispatching capacity is relatively sufficient. And the tracking errors of scenario C are within the expectations. Thus, it can be verified that the tracking error in this model is determined by the values of r_1 and r_2 when the dispatching capacity is sufficient.

A negative error means that the Agg imports more electricity in the day-ahead market than it actually consumes. In fact, this type of phenomenon is not accidental. To cope with the uncertainties of PV output, the Agg considers the worst case and imports a surplus amount of electricity in the day-ahead market, resulting in a negative error when the PV output is not in the worst case and the dispatching capacity of the EVs is insufficient. However, sufficient electricity can be ensured if the PV output is in the worst case. This strategy avoids the risk of the Agg in purchasing the electricity in the real-time electricity market when the dispatching capacity of EVs is insufficient.

The tracking accuracies obtained from the simulation results are shown in Table VI. With an increasing value of barrier factors, the tracking accuracy decreases. In all simulation scenarios, the tracking accuracies are higher than 95%. As a high tracking accuracy can be achieved in the real-time scheduling phase, the Agg can avoid being punished for the deviation between the day-ahead settlement and actual electricity consumption in all of the simulation scenarios.

TABLE VI
TRACKING ACCURACY OF AGG IN REAL-TIME OPERATION

Scenario	Accuracy (%)
A	99.90
B	99.58
C	96.46
D	99.52

To verify the effects of the barrier factors on each EV, the SOC of four randomly-selected EVs are compared and analyzed for scenario A and scenario C.

Figure 10 illustrates the respective SOC changes of the four EVs over all the scheduling times. Although the selected EVs are different as the initial SOC and initial scheduling time, the change range of the SOC in scenario C is smaller than that in scenario A for all EVs. As shown in (32), the change in the SOC decreases when the charging and discharging power is suppressed by large values of barrier factors. However, no matter how the values of the barrier factors change, the SOC value of an EV leaving during the dispatching period will meet the demand of the user (0.85) because of constraint (34).

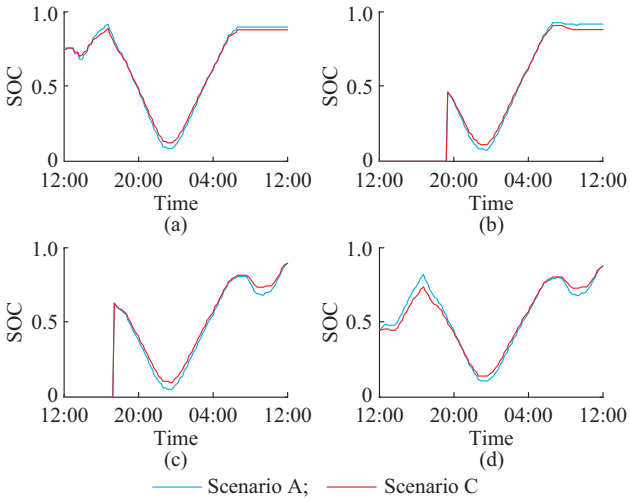

Fig. 10. SOC of each EV. (a) EV78. (b) EV38. (c) EV69. (d) EV94.

In actual operation, the values of r_1 and r_2 can be set to larger values which satisfy the requirements for tracking accuracy. To ensure tracking accuracy, the over-charging and over-discharging of EVs can be restrained, and the satisfaction of EV users participating in dispatching can be improved.

V. CONCLUSION

This paper presents a day-ahead and real-time energy management strategy for an Agg to manage internal sources under the uncertainties of PV output. In particular, a day-ahead RO model and a rolling horizon optimization based real-time convex optimization model are respectively established. Case studies validate that the day-ahead scheduling is robust. The economic operation of the Agg in real-time can be guaranteed, even if the PV output is in a worst-case scenario. The rolling horizon optimization based convex optimization in real-time operation is more efficient and convenient for determining the EV dispatching power, because of the relaxation of the non-convex constraints. The tracking error of the day-ahead scheduled power plan is controllable when the dispatching EV capacity is sufficient, and the convex optimization model can restrain the over-charging and over-discharging of EVs.

REFERENCES

[1] L. Hattam and D.V. Greetham, "Green neighbourhoods in low voltage networks: measuring impact of electric vehicles and photovoltaics on load profiles," *Journal of Modern Power Systems and Clean Energy*, vol. 5, no. 1, pp. 105-116, Jan. 2017.

[2] S. Valero, M. Ortiz, C. Senabre *et al.*, "Methods for customer and demand response policies selection in new electricity markets," *IET Generation, Transmission & Distribution*, vol. 1, no. 1, pp. 104-110, Jan. 2007.

[3] S. P. Durrani, S. Balluff, L. Wurzer *et al.*, "Photovoltaic yield prediction using an irradiance forecast model based on multiple neural networks," *Journal of Modern Power Systems and Clean Energy*, vol. 6, no. 2, pp. 255-267, Mar. 2018.

[4] B. Khorramdel, C. Y. Chung, N. Safari *et al.*, "A fuzzy adaptive probabilistic wind power prediction framework using diffusion kernel density estimators," *IEEE Transactions on Power Systems*, vol. 33, no. 6,

pp. 7109-7121, Nov. 2018.
[5] D. Arunima and D. Sanjoy, "Frequency regulation in deregulated market using vehicle-to-grid services in residential distribution network," *IEEE Systems Journal*, vol. 12, no. 3, pp. 2812-2820, Sept. 2018.
[6] Z. Yang, K. Li, Q. Niu *et al*., "A self-learning TLBO based dynamic economic/environmental dispatch considering multiple plug-in electric vehicle loads," *Journal of Modern Power Systems and Clean Energy*, vol. 2, no. 4, pp. 298-307, Dec. 2014.
[7] M. Pantoš, "Stochastic optimal charging of electric-drive vehicles with renewable energy," *Energy*, vol. 36, no. 11, pp. 6567-6576, Nov. 2011.
[8] C. Jin, J. Tang, and P. Ghosh. "Optimizing electric vehicle charging: a customer's perspective," *IEEE Transactions on Vehicular Technology*, vol. 62, no. 7, pp. 2919-2927, Sept. 2013.
[9] S. Pirouzi, J. Aghaei, and V. Vahidinasab *et al*., "Robust linear architecture for active/reactive power scheduling of EV integrated smart distribution networks," *Electric Power Systems Research*, vol. 155, pp. 8-20, Feb. 2018.
[10] J. Soares, Z. Vale, N. Borges *et al*., "Multi-objective robust optimization to solve energy scheduling in buildings under uncertainty," in *Proceedings of 19th International Conference on Intelligent System Application to Power Systems (ISAP)*, San Antonio, USA, Sept. 2017, pp. 1-6.
[11] Q. Huang, Q. Jia, Z. Qiu *et al*., "Matching EV charging load with uncertain wind: a simulation-based policy improvement approach," *IEEE Transactions on Smart Grid*, vol. 6, no. 3, pp. 1425-1433, May 2015.
[12] N. Liu, Q. Chen, J. Liu *et al*., "A heuristic operation strategy for commercial building microgrids containing EVs and PV system," *IEEE Transactions on Industrial Electronics*, vol. 62, no. 4, pp. 2560-2570, Apr. 2015.
[13] Q. Chen, F. Wang, B. Hodge *et al*., "Dynamic price vector formation model-based automatic demand response strategy for PV-assisted EV charging stations," *IEEE Transactions on Smart Grid*, vol. 8, no. 6, pp. 2903-2915, Nov. 2017.
[14] R. Wang, P. Wang, G. Xiao *et al*., "Two-stage mechanism for massive electric vehicle charging involving renewable energy," *IEEE Transactions on Vehicular Technology*, vol. 65, no. 6, pp. 4159-4171, Jun. 2016.
[15] H. Yang, H. Pan, F. Luo *et al*., "Operational planning of electric vehicles for balancing wind power and load fluctuations in a microgrid," *IEEE Transactions on Sustainable Energy*, vol. 8, no. 2, pp. 592-604, Apr. 2017.
[16] N. Erdogan, F. Erden, and M. Kisacikoglu, "A fast and efficient coordinated vehicle-to-grid discharging control scheme for peak shaving in power distribution system," *Journal of Modern Power Systems and Clean Energy*, vol. 6, no. 3, pp. 555-566, May 2018.
[17] R. Jiang, M. Zhang, G. Li *et al*., "Two-stage robust power grid optimization problem," in *Proceedings of 62nd IIE Annual Conference and Expo*, Orlando, USA, May 2012, pp. 885-893.
[18] S. Hanif, H. B. Gooi, T. Massier *et al*., "Distributed congestion management of distribution grids under robust flexible buildings operations," *IEEE Transactions on Power Systems*, vol. 32, no. 6, pp. 4600-4613, Nov. 2017.
[19] R. Xu, C. Zhang, Y. Xu *et al*., "Rolling horizon based multi-objective robust voltage/var regulation with conservation voltage reduction in high PV-penetrated distribution networks," *IET Generation, Transmission & Distribution*, vol. 13, no. 9, pp. 1621-1629, May 2019.
[20] G. Wenzel, M. Negrete-Pincetic, D. E. Olivares *et al*., "Real-time charging strategies for an electric vehicle aggregator to provide ancillary services," *IEEE Transactions on Smart Grid*, vol. 9, no. 5, pp. 5141-5151, Sept. 2018.
[21] B.Y. Liaw, M. Dubarry, V. Svoboda *et al*., "Capacity and power fading mechanism identification from a commercial cell evaluation," *Journal of Power Sources*, vol. 165, no. 2, pp. 566-572, Mar. 2007.
[22] Z. Liu, Q. Wu, M. Shahidehpour *et al*., "Transactive real-time electric vehicle charging management for commercial buildings with PV onsite generation," *IEEE Transactions on Smart Grid*, vol. 10, no. 5, pp. 4939-4950, Sept. 2019.

Junjie Hu received the M.Sc. degree in control theory and control engineering from Tongji University, Shanghai, China, in 2010, and the Ph.D. degree in electrical engineering from the Technical University of Denmark, Copenhagen, Denmark, in 2014. He was a Postdoctoral Researcher with the Department of Electrical Engineering, Technical University of Denmark. He is currently an Associate Professor with the School of Electrical and Electronic Engineering, North China Electric Power University, Beijing, China. His current research interests include distributed energy resources energy management, transactive energy and their participations in prosumer energy management, and multi-energy system optimization.

Huayanran Zhou received the B.S. degree in electrical engineering and automation from North China Electric Power University, Baoding, China, in 2018. She is currently pursuing the master's degree with the School of Electrical and Electronic Engineering, North China Electric Power University, Beijing, China. Her research interests include distributed energy resources energy management, transactive energy and their participations in prosumer energy management, and multi-energy system optimization.

Yang Li received the B.S. degree in electrical engineering and automation from Yanshan University, Yanshan, China, in 2017. She is currently pursuing the master's degree with the School of Electrical and Electronic Engineering, North China Electric Power University, Beijing, China. Her research interests include distributed energy resources energy management, transactive energy and their participations in prosumer energy management, and multi-energy system optimization.

Peng Hou received the B.Eng. degree in electrical engineering from Hebei University of Technology, Tianjin, China, in 2008, the M.Sc. degree in electrical engineering from Chalmers University of Technology, Gothenburg, Sweden, in 2010, and the Ph.D. degree in wind power technology from Aalborg University, Aalborg, Denmark, in 2017. He is currently a Lead R&D at SEWPG European Innovation Center, Aarhus, Denmark. His research interests include offshore wind farm planning, virtual power plant aggregator, power distribution system, smart home, transactive energy, integrated energy system, renewable energy based hydrogen production, electricity market analysis, and applications of optimization theory in these areas.

Guangya Yang received Ph. D. degree in 2008 from the University of Queensland, St Lucia, Australia, in the field of electrical power systems. Currently, he is a senior power system engineer with Ørsted and Senior Scientist with Technical University of Denmark, Copenhagen, Denmark. Since 2009, he has been developing and leading many industrial collaborative projects in Denmark. He is editorial board member of IEEE Transactions on Sustainable Energy, IEEE Transactions on Power Delivery, IEEE Access, and Journal of Modern Power Systems and Clean Energy. His research interests include power system dynamic security and protection, offshore wind power system design and control, and transactive energy applied to distributed energy resources.